

Dual-wavelength noiselike pulse generation via polarization rotation and stimulated Raman scattering in an erbium-doped fiber ring laser

Thibault North and Martin Rochette

Department of Electrical and Computer Engineering, McGill University, Montréal (Québec),
H3A 2A7, Canada

ABSTRACT

We demonstrate the generation of dual-wavelength noiselike pulses in an Er^{3+} fiber laser. A ring cavity configuration including a polarizer as saturable absorber induces a first series of pulses at the wavelength of 1550 nm via nonlinear polarization rotation. From the Raman gain of these pump pulses emerges a second series of Stokes pulses at 1650 nm. With an adequate control of the polarization states in the cavity, the Stokes pulses contain 67% of the total energy and reach a bandwidth of 84 nm in the U-band.

Keywords: Raman effect, nonlinear polarization rotation, noise-like pulses, erbium-doped fiber laser

1. INTRODUCTION AND PREVIOUS WORK

Fiber ring cavities including a saturable absorber such as nonlinear polarization rotation (NPR) or semiconductors are known to generate ultrashort pulses from the spontaneous emission of the gain medium placed inside the cavity.^{1,2} Furthermore, these ring cavities can often sustain another kind of pulses, in a regime usually referred to as the noiselike pulse (NLP) regime. Instead of soliton-like pulses, the cavity spawns wave packets composed of a picosecond envelope comprising femtosecond-scale oscillations.^{3,4} The formation of such pulses was attributed to several nonlinear effects and interactions, without consensus so far, and is known to be influenced by the saturable absorber, birefringence, self- and cross-phase modulation, four wave mixing, and soliton self-frequency shift.⁵⁻⁸ Spectrally, the averaging of noiselike pulses results in a smooth and wide spectrum, that typically spreads over more than 10 nm full width at half maximum (FWHM). In the time-domain, a typical gaussian pedestal of several picoseconds superimposed by a sharp peak of a width in the femtosecond range can be observed, as expected for the autocorrelation of noise. In a recent publication, Vazquez-Zuniga et al. attained a record bandwidth of 135 nm in a ring cavity including a segment of highly nonlinear fiber (HNLF) in normal dispersion.⁹ The flat supercontinuum formed by noiselike pulses in their cavity extends towards the long wavelengths up to 1650 nm via stimulated Raman scattering (SRS). Applications in low-coherence interferometry were demonstrated with the characterization of fiber Bragg gratings,^{10,11} optical data storage,¹² temperature distribution measurements,¹³ as well as the generation of supercontinuum.^{8,14} As of today, only one paper features the dual-wavelength operation of a laser in NLP regime. It was attributed to birefringence-induced loss modulation, and was demonstrated using a 450 m long silica cavity, with a spectral offset of 25 nm.⁴

We report the observation of a new dual-wavelength fiber ring laser operating in NLP regime. A first series of pulses are generated at a wavelength of ~ 1550 nm, the Raman pump (RP) pulses, from amplified spontaneous emission (ASE) of an erbium-doped fiber and the effect of NPR. Stokes pulses are generated from a Raman effect at a wavelength of ~ 1650 nm, corresponding to a 13.2 THz offset from the RP pulses. A cavity configuration presented by Vazquez-Zuniga et Jeong,⁹ SRS is increased by the addition of a HNLF in normal dispersion, resulting in a flat supercontinuum. We demonstrate that the effect of SRS can be reinforced by taking advantage of a nonlinearity increased by a factor of 100. Instead of extending the bandwidth of the existing RP pulses,

Further author information: (Send correspondence to Martin Rochette)

Martin Rochette: E-mail: martin.rochette@mcgill.ca,

Thibault North: E-mail: thibault.north@mail.mcgill.ca

broadband and powerful noiselike pulses are spawned beyond 1650 nm, outside the amplification region of Er^{3+} -doped silica fibers. Two operating regimes are presented. In the first regime, the RP pulses efficiently generate Stokes pulses, that exceed the RP power by 2.5 dB. In the second regime, a flat supercontinuum spreading over 84 nm is observed at the Stokes wavelengths, while the RP pulses extend over 47 nm at 1550 nm. To the best of our knowledge, there is no previous report of the operation of an Er^{3+} laser in NLP regime beyond 1650 nm.^{3-5,9,14}

2. EXPERIMENTAL SETUP

Fig. 1 schematizes the experimental setup. Its ring cavity is similar to the ones used for mode-locking by NPR.¹

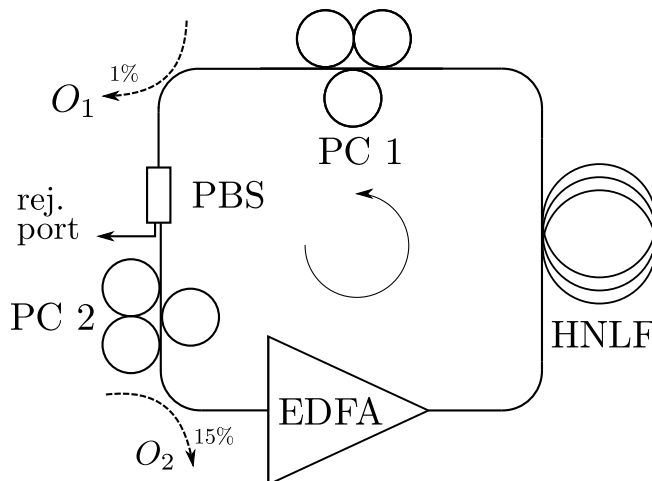


Figure 1. Ring cavity composed of a HNLf, an EDFA, two PCs, a PBS and two output tap couplers $O_{1,2}$. EDFA: erbium-doped fiber amplifier, PC: polarization controller, PBS: polarization beam splitter.

The setup includes a 1007 m long HNLf with a nonlinear waveguide coefficient $\gamma = 11.5 \text{ W}^{-1}\text{km}^{-1}$, a chromatic dispersion coefficient $D = -0.71 \text{ ps nm}^{-1}\text{km}^{-1}$, and a loss of 1.5 dB at a wavelength of 1550 nm. The erbium-doped fiber amplifier (EDFA) containing an optical isolator and pumped at 976 nm has a length \times chromatic dispersion product of $LD_{\text{EDFA}} = 138 \text{ ps nm}^{-1}$. The average chromatic dispersion in the cavity is normal with a value of $LD_{\text{avg}} = -406 \text{ ps nm}^{-1}$ due to the presence of the other components, representing ~ 20 m of silica single mode fiber. The two outputs couplers $O_{1,2}$ of 1% and 15%, respectively, are connected to an optical spectrum analyzer and a photodiode for monitoring purposes. A linearly polarized laser output of high output coupling ratio is available at the rejection port of the cavity, as the second output of the polarization beam-splitter (PBS).

3. RESULTS

The source self-ignites noiselike pulses with an EDFA pump power above ~ 100 mW and an adjustment of the two polarization controllers (PCs). Visible via the output of a fast photodiode, the sudden apparition of a burst of pulses at 194 kHz translates in the frequency domain as the apparition of a smooth and broadband spectrum from the initial continuous-wave regime. In Fig. 2(a) and (b), the spectrum corresponding to the two main operation regimes are observed from output O_2 , and the time-domain output is shown in the corresponding insets.

3.1 Operation regimes

In the first regime of Fig. 2(a), a pulsed operation around 1550 nm results from an adequate PC tuning. At low EDFA pump power, a weak signal generated from SRS and noted (i) is observed at 1670 nm. With a further increase of the EDFA pump power, the power of the Stokes signal increases faster than the power of the RP

pulses. With a careful adjustment of the PCs, noiselike Stokes pulses exceeding the power of the RP pulses are then sustained in the cavity.

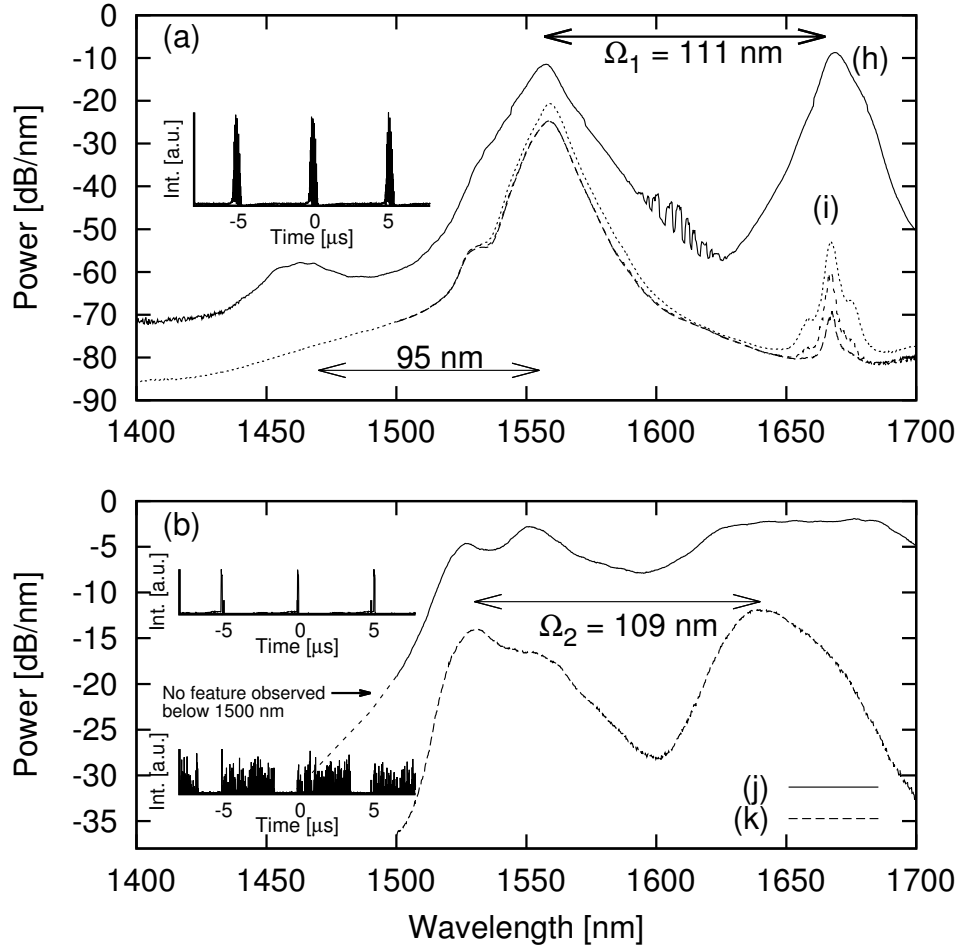


Figure 2. Dual-wavelength lasing at O₂: (a) at various EDFA pump powers. Inset: photodiode response of the RP pulses of trace (h). (b) Other PC configurations. The spectral offset between the pump and the Stokes pulses are denoted by $\Omega_{1,2}$. Insets: corresponding photodiode intensity response.

We believe that the red-most signal is sustained by a Raman gain supplied by the 1550 nm signal. Indeed, a wavelength separation of $\Omega_1 = 111$ nm corresponds well to the offset of 13.2 THz that is expected for a Stokes wave due to a SRS process in silica. In trace (h), the Stokes pulses generated from SRS contain 1.5 times more energy than the RP pulses, and spread over 8.4 nm while the RP pulses have a bandwidth of 10 nm. The peak observed at a wavelength of 1464 nm in Fig. 2(a) is attributed to a Raman anti-Stokes wave for its consistent offset with respect to the wavelength of the RP pulses. A spectral separation of 95 nm again corresponds well to 13.2 THz, and the 50 dB difference with the RP pulses is expected because of a much less probable phase-matching of the anti-Stokes wave.¹⁵ The asymmetry in amplitude of the Stokes and anti-Stokes line suggests that the gain observed at the Stokes wavelength originates from a SRS process rather than the effect of degenerate four-wave mixing of the RP pulses. The complex structure of noiselike pulses prevents an exact measurement of their peak power due to the finite time response of electrical photodiodes. However, NLPs of Fig. 2(a) exceed the expected Raman threshold $P_{th} = 16A_{Eff}/(g_R L_{Eff}) = 14.5$ W, with $g_R = 6.5 \times 10^{-14}$ m W⁻¹, $L_{Eff} = 850$ m, and $A_{Eff} \sim 50 \mu\text{m}^2$ for the HNLF.¹⁵ This value is a lower bound to the actual NLPs peak power, and the absence of an anti-Stokes line in Fig. 2(b) suggests that their peak power is lower than that of pulses in (a).

Other positionings of the PCs yield to a different NLP regime and two subregimes, shown in Fig. 2(b). Again,

noiselike pulses are observed at two different wavelengths with a spectral offset $\Omega_1 \simeq \Omega_2$ corresponding to a SRS process. The bandwidth for the RP and Stokes pulses are of 34 nm and 32 nm respectively for the subregime (k). In this configuration, the Stokes pulses contain 1.65 the average power of the RP pulses. With a careful tuning of the PCs, the bandwidth of the RP and Stokes pulses is altered⁷ and leads to subregime (j). The Stokes pulses now spread over a bandwidth of 84 nm FWHM, while the RP pulses are of 46 nm FWHM.

3.2 Effect of the variation of the EDFA pump power

In this subsection, we focus on what is found to be the most stable subregime. Denoted (k) and depicted in Fig. 2(b), it is often the first one observed when pulsing starts. The output power at O_2 and at the rejection port are presented in Fig. 3(a) as the EDFA pump power is altered. It was observed that the rejection power presents an OCR of 50% at any EDFA pump power. In (b), the increase of the EDFA pump power first leads to the spectral broadening of the RP pulses. A saturation point is then reached at ~ 150 mW, a point after which the Stokes pulses start broadening as well and consume the additional power of the RP pulses provided by the gain medium. The autocorrelation width of the RP pulses does not significantly change after saturation, as opposed to the behaviour reported by Vazquez-Zuniga and Jeong.⁹ In their work, the existing NLPs take advantage of the excess of EDFA pump power and broaden temporally without sign of saturation. Again, the observed behaviour suggests an efficient transfer of power towards the Stokes pulses via SRS. In (c), the EDFA pump power is

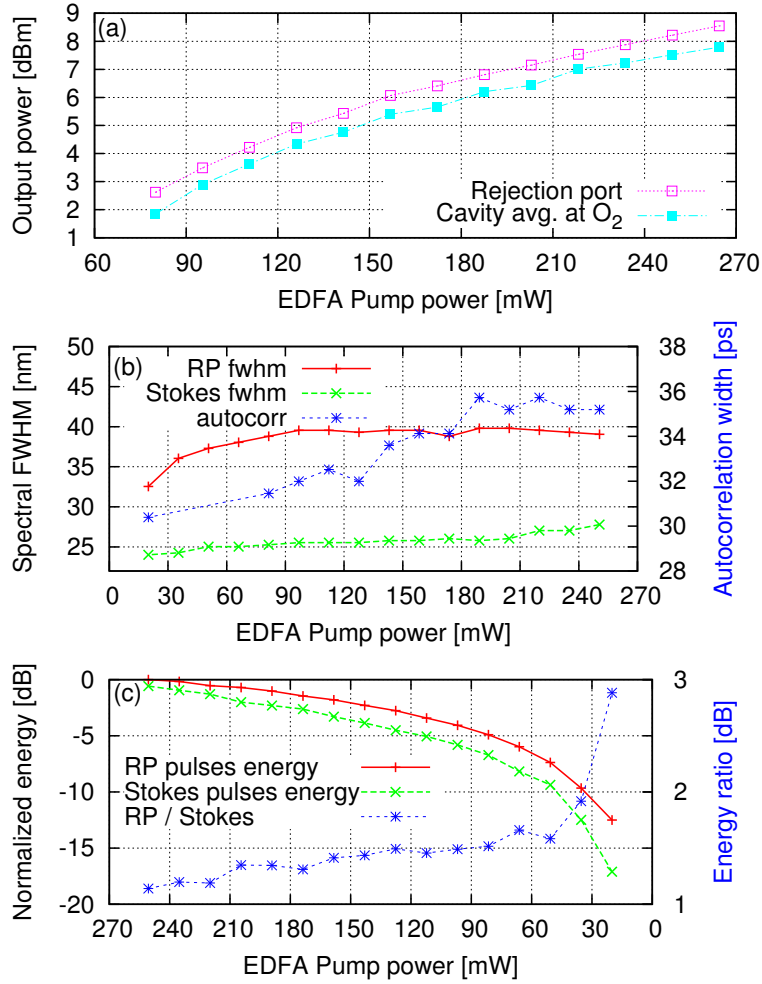


Figure 3. Effects of a variation of the EDFA pump power. (a) Power at the rejection port and in the cavity, observed from output coupler O_2 . (b) Spectral width at the RP and Stokes pulses, and autocorrelation width for the RP pulses. (c) Pulses' spectral energy as the EDFA pump power is decreased.

decreased, and the energy contained in each of the RP and Stokes pulses represented, along with the energy ratio between them. Because the Raman response is quasi-instantaneous,¹⁵ the Stokes pulses are sustained only as long as the RP pulses keep a sufficient peak power. In accordance with time-domain observation, the peak power of RP pulses diminishes with the EDFA pump power, which quickly lowers the Raman gain. The Stokes pulses therefore lose energy faster than the RP pulses, sustained directly by the gain medium.

3.3 Time-domain output

In the time-domain, the spectrogram of RP pulses of Fig. 2(a) captured by a frequency-resolved optical gating (FROG) is shown in Fig. 4. The ratio between the autocorrelation peak and the shoulder of the pulse's autocorrelation is close to 2, which indicates the absence of structure in the pulse, as discussed for example in Refs.^{3,8}

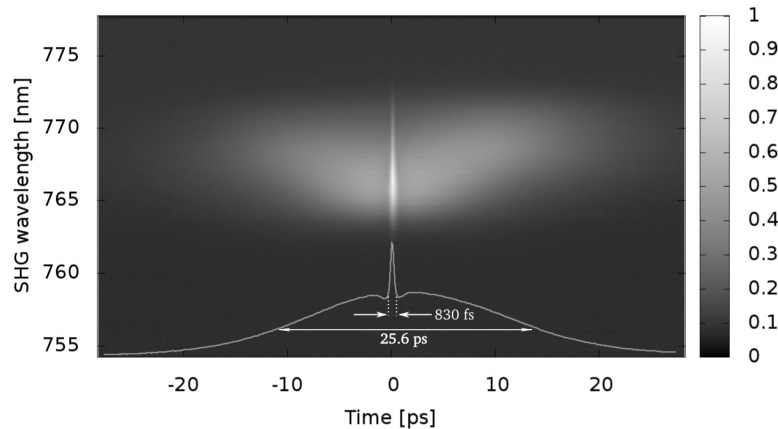


Figure 4. FROG spectrogram of a noiselike pulse and its autocorrelation width of 25.6 ps.

Two main regimes are observed at the repetition rate of the cavity, 194 kHz. First, “square-shaped” pulses, also seen in,⁹ are broadening with increasing EDFA pump power.

Traveling mostly in a fiber with normal dispersion, The RP and Stokes pulses do not propagate at the same group velocity. In 1 km of HNLF, this mismatch accounts for 4 ns, but this delay is compensated by the fact that Stokes pulses experience an asymmetrical gain and loss profile, induced by the slower RP pulses. This was confirmed by an alternative filtering of the RP and Stokes pulses. The second regime shown in Fig. 5 indicates $\sim 3.5 \mu\text{s}$ long bursts which contains a set of impulses separated by $\sim 33 \text{ ns}$. Regardless of the EDFA pump power, a frequency analyzer indicates the presence of a peak at the fundamental frequency along with another peak at 30 MHz. The overall burst duration and peak power decreases with a decreasing EDFA pump power. Stokes

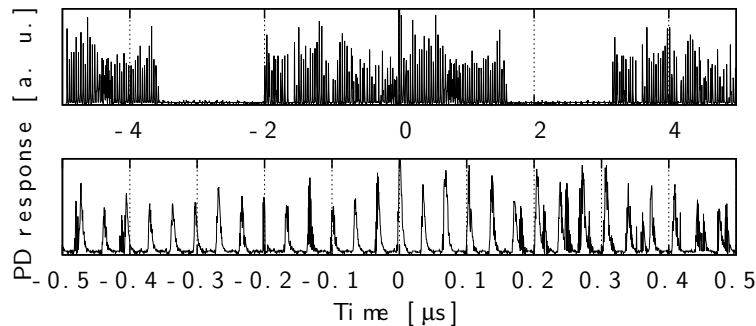


Figure 5. Time-domain behaviour at two different time scales. PD: photodiode.

pulses are sustained up to the point of total extinction of the source, because of the presence of a powerful RP

pulse. In this process, it is observed that the RP pulses spectrally splits into two components with an offset of 8 nm. Pulses sliding along each other are then visible, as previously observed.⁴ A significant birefringence of $\Delta n = 3.5 \times 10^{-7}$ in the HNLF and the additional polarization group delay induced by the PBS are likely to be responsible for this phenomenon.

4. CONCLUSION

A dual wavelength all-fiber ring laser based on NPR is demonstrated to operate in NLP regime. Operating in normal dispersion, RP pulses are observed in the C-band and at the first Stokes wavelength in the U-band. The bandwidth of these pulses can be adjusted by a tuning of the PCs, and a broadband continuum of 84 nm is obtained at the Stokes pulses, up to 1700 nm. This region stands in the gap between the emission regions of erbium and thulium, and is therefore interesting for applications. Despite its fundamental repetition rate of 194 kHz, the cavity can sustain bursts of NLPs extending over the whole cavity period with an increased EDFA pump power and with little changes to the spectrum. Finally, a large OCR of 50% provides an output power of 8 dBm that is linearly polarized.

ACKNOWLEDGMENTS

The authors are thankful to Pierre Galarneau and Stéphane Bourquin for insightful comments, and the National Optics Institute (INO) in Quebec city for their financial support.

REFERENCES

- [1] Matsas, V., Newson, T., and Zervas, M., “Self-starting passively mode-locked fibre ring laser exploiting nonlinear polarisation switching,” *Optics communications* **92**(1-3), 61–66 (1992).
- [2] Set, S. Y., Yaguchi, H., Tanaka, Y., and Jablonski, M., “Laser Mode Locking Using a Saturable Absorber Incorporating Carbon Nanotubes,” *J. Lightwave Technol.* **22**, 51 (Jan 2004).
- [3] Horowitz, M., Barad, Y., and Silberberg, Y., “Noiselike pulses with a broadband spectrum generated from an erbium-doped fiber laser,” *Opt. Lett.* **22**, 799–801 (Jun 1997).
- [4] Horowitz, M. and Silberberg, Y., “Control of noiselike pulse generation in erbium-doped fiber lasers,” *Photonics Technology Letters, IEEE* **10**, 1389–1391 (oct. 1998).
- [5] Kang, J., “Broadband quasi-stationary pulses in mode-locked fiber ring laser,” *Optics communications* **182**(4-6), 433–436 (2000).
- [6] Zhao, L., Tang, D., Cheng, T., Tam, H., and Lu, C., “120 nm Bandwidth noise-like pulse generation in an erbium-doped fiber laser,” *Optics Communications* **281**(1), 157–161 (2008).
- [7] Pottiez, O., Grajales-Coutiño, R., Ibarra-Escamilla, B., Kuzin, E. A., and Hernández-García, J. C., “Adjustable noiselike pulses from a figure-eight fiber laser,” *Appl. Opt.* **50**, E24–E31 (Sep 2011).
- [8] Hernandez-Garcia, J., Pottiez, O., Estudillo-Ayala, J., and Rojas-Laguna, R., “Numerical analysis of a broadband spectrum generated in a standard fiber by noise-like pulses from a passively mode-locked fiber laser,” *Optics Communications* **285**(7), 1915–1919 (2012).
- [9] Vazquez-Zuniga, L. A. and Jeong, Y., “Super-Broadband Noise-Like Pulse Erbium-Doped Fiber Ring Laser With a Highly Nonlinear Fiber for Raman Gain Enhancement,” *Photonics Technology Letters, IEEE* **24**, 1549–1551 (sept.1, 2012).
- [10] Keren, S. and Horowitz, M., “Interrogation of fiber gratings by use of low-coherence spectral interferometry of noiselike pulses,” *Opt. Lett.* **26**, 328–330 (Mar 2001).
- [11] Keren, S., Rosenthal, A., and Horowitz, M., “Measuring the structure of highly reflecting fiber Bragg gratings,” *Photonics Technology Letters, IEEE* **15**, 575–577 (april 2003).
- [12] Keren, S., Brand, E., Levi, Y., Levit, B., and Horowitz, M., “Data storage in optical fibers and reconstruction by use of low-coherence spectral interferometry,” *Opt. Lett.* **27**, 125–127 (Jan 2002).
- [13] Goloborodko, V., Keren, S., Rosenthal, A., Levit, B., and Horowitz, M., “Measuring Temperature Profiles in High-Power Optical Fiber Components,” *Appl. Opt.* **42**, 2284–2288 (May 2003).
- [14] Takushima, Y., Yasunaka, K., Ozeki, Y., and Kikuchi, K., “87 nm bandwidth noise-like pulse generation from erbium-doped fibre laser,” *Electronics Letters* **41**, 399–400 (march 2005).
- [15] Agrawal, G., [Nonlinear fiber optics], *Optics and Photonics*, Academic Press (2007).